



Cite this: *Sustainable Food Technol.*, 2025, **3**, 1610

## Reverse osmosis and forward osmosis concentration of cranberry juice: processing effects on juice quality

Mark Emile H. Punzalan and Olga I. Padilla-Zakour \*

Reverse (RO) and forward osmosis (FO) are membrane processes that are alternatives to thermal evaporation, operating at room or lower temperature during concentration of liquid foods, using less energy and retaining heat-labile components. Pasteurized cranberry juice (5.5° Brix, pH 2.6) was concentrated by RO at 3.5 MPa and 25 °C to 17.8° Brix and further concentrated by FO at 25 °C to 52.3° Brix. Potassium citrate (2.35 mol L<sup>-1</sup>) was used as FO draw solution. Samples were stored refrigerated at 4 °C for 6 months. Total soluble solids, pH, water activity, titratable acidity, citric and malic acids, CIE color, % polymeric color, total phenolics, flavonoids, monomeric anthocyanins, DPPH and ABTS antioxidant activities were measured on concentrated and/or reconstituted samples before and after processing and monthly for 6 months. Total plate and yeast and mold counts were evaluated before and after FO processing and after 1, 3, and 6 months on concentrated samples. Results showed that during RO, anthocyanins decreased by 4% while FO induced no significant changes ( $p > 0.05$ ) in the physicochemical properties. During storage, color values in the RO + FO concentrate decreased significantly ( $p < 0.05$ ), with a total color change ( $\Delta E$ ) of  $10.4 \pm 0.9$  at the end of 6 months. Polymeric color increased 2-fold while anthocyanins and DPPH Trolox equivalents decreased by 57% and 23% respectively after 6 month storage. Total phenolics, flavonoids and ABTS antioxidant activity were retained after RO and FO and through storage time. Total plate count was  $<1.5 \log \text{CFU mL}^{-1}$  before and after FO processing and after storage. No yeast and molds were detected. These findings suggested that a combined RO + FO can produce high-quality cranberry juice concentrate that retains quality attributes and bioactive components but may need frozen storage for preservation of anthocyanins.

Received 8th April 2025  
Accepted 7th August 2025

DOI: 10.1039/d5fb00142k  
[rsc.li/susfoodtech](http://rsc.li/susfoodtech)

### Sustainability spotlight

Using reverse osmosis (RO) and forward osmosis (FO) as a concentration technology for fruit juices aligns with the goal of ensuring sustainable consumption and production patterns. Compared to thermal evaporation, which is the typical juice concentration process, RO and FO are less energy-intensive. By using RO, energy usage can be reduced by up to 90% and using FO can lower greenhouse emissions by up to 94%. In our work, we concentrated cranberry juice using a combined RO and FO process, resulting in a concentrate that retains overall quality and health-promoting heat-sensitive components present in the original juice. Therefore, we can significantly improve the sustainability of the concentration process without excessive heat input while maintaining product quality.

## 1 Introduction

Cranberry juice is a valued commodity due to its health benefits. Several studies have demonstrated that cranberry juice can be advantageous for urinary tract health<sup>1</sup> and may offer anti-cancer and anti-inflammatory properties<sup>2</sup> due to its proanthocyanidin and flavonoid content. It also has antioxidant activities due to the presence of polyphenols, ascorbic acid and triterpenes.<sup>3-5</sup> However, the processing methods to produce juices can influence the retention of these bioactive compounds.<sup>6</sup>

Juice is prepared in several ways. It can be a fresh extract, pasteurized, mixed with other juices or concentrated. Juice concentrates available commercially are conventionally prepared by thermal evaporation. Although the processing conditions during evaporation render the product safe by inactivating microorganisms, the exposure of the juice to higher temperatures for a long residence time degrades the heat-labile components such as bioactive phenolic components and volatile compounds responsible for aroma and flavor.<sup>7,8</sup> In a study by Côté *et al.* (2011),<sup>9</sup> the cranberry juice concentrate produced through vacuum evaporation retained 11% and 6% of the total phenolic content compared to the level in the juice after pressing and clarification, respectively, before evaporation. To minimize the negative effects of heat and better preserve the

Department of Food Science, Cornell AgriTech, Geneva, NY, USA 14456. E-mail: [oop1@cornell.edu](mailto:oop1@cornell.edu)



juice qualities, nonthermal approaches in concentrating juices were studied, which include freeze concentration and membrane concentration processes. In freeze concentration (FC), the water in the fruit juice is frozen to form ice crystals which are then separated from the liquid, resulting in a concentrated solution. FC produces high-quality juice and consumes less energy than thermal evaporation, but it is an expensive, technically complex, and slow process.<sup>10,11</sup> Some components are also lost, trapped in the ice crystals.<sup>12</sup>

Other alternative technologies for concentration that operate at room temperature or lower are membrane concentration processes such as reverse osmosis (RO) and forward osmosis (FO). RO applies external pressure to force the water to pass through a semi-permeable membrane.<sup>13</sup> The applied pressure must be high enough to counteract the osmotic pressure exhibited by the feed, especially when the feed becomes more concentrated as the process progresses. For an effective RO process, transmembrane pressure (TMP) is one of the critical factors. Variable levels of TMP during the concentration of apple juice<sup>14</sup> and grape juice<sup>15</sup> ranging from 2.5 to 7.0 MPa were investigated, suggesting that an increase in permeate fluxes can be achieved by increasing the TMP. RO is advantageous over thermal concentration due to its low processing temperature, low energy consumption,<sup>16,17</sup> and high permeate fluxes, making it a suitable concentration process but it can be challenging due to pronounced fouling and concentration polarization.<sup>18</sup> This limits the use of RO as a pre-concentration step since the total soluble solids content that it can achieve is less than that of thermal evaporation. Several studies on RO applied to fruit juices obtained a total soluble solids content ranging from 20 to 36° Brix, although high pressure, up to 7000 kPa, was required.<sup>19–25</sup> For cranberry juice and blends, RO was used as a pre-concentration step to achieve 15° Brix soluble solids.<sup>13,26</sup>

To reach higher concentrations in an efficient manner, other technologies will be required. FO represents an option as it concentrates liquid foods by drawing the water from the food using a draw solution (DS) and a semi-permeable membrane. The osmotic pressure gradient between the feed and the DS acts as the driving force, eliminating the need for external pressure application compared to the RO process. The DS is a key component of FO, thus it must have a higher osmotic pressure compared to the feed. For fruit juice concentration, the DS must be food grade and able to provide high water and low reverse solute fluxes.<sup>27,28</sup> In previous works, juices processed by FO using sodium chloride as DS included apple juice,<sup>29</sup> grape juice,<sup>30</sup> pomegranate juice,<sup>31</sup> and sugarcane juice,<sup>32</sup> achieving total soluble solids concentration of up to 60° Brix. Aside from sodium chloride, there are other materials used as DS to minimize the impact of reverse solute flux in terms of flavor profile and juice quality, including sugars (glucose, sucrose), organic acids (citric acid), salts (potassium sorbate, potassium lactate, sodium benzoate, sodium lactate, sodium citrate), and other food additives.<sup>33–36</sup>

FO is more advantageous than thermal concentration due to low operating temperatures that maintain juice quality.<sup>37</sup> FO is less susceptible to fouling compared to other pressure-driven membrane separation processes,<sup>38</sup> allowing higher juice

concentration than RO.<sup>39</sup> However, when compared to RO, one drawback of FO is that it is a relatively slow process due to lower fluxes. The development of a sequential RO + FO process can render a high-quality nonthermally concentrated juice at targeted soluble solids content with improved efficiency. There have been no published reports on using RO followed by FO for cranberry juice concentration. The sequential RO + FO process could address the unique challenges of cranberry juice concentration due to the juice's low pH, while retaining the bioactive compounds. Therefore, this study researched the feasibility of a novel sequential RO and FO concentration process for cranberry juice, and evaluating product quality and microbial stability during 6 months of refrigerated storage.

## 2 Materials and methods

### 2.1 Reverse osmosis (RO) concentration

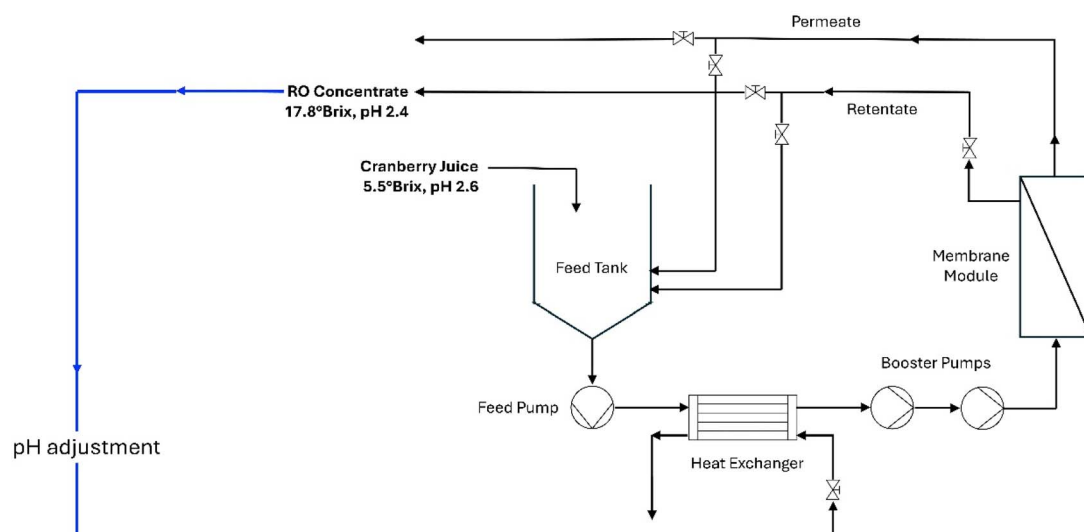
The schematic diagram of RO is shown in Fig. 1a. The RO experiments were conducted using the Alfa Laval PilotUnit Multi Filtration system equipped with a RO98 pH<sup>TM</sup> spiral-wound membrane (Alfa Laval Inc., Richmond, VA, USA) at the Seneca Foods Foundation Pilot Plant, Cornell AgriTech, Geneva, NY, USA. The membrane has a filtration area of 4.5 m<sup>2</sup> and has  $\geq 98\%$  rejection rate measured using 2000 mg L<sup>-1</sup> NaCl solution at 1.6 MPa and 25 °C. All parameter adjustments were controlled, and data were recorded and acquired through the built-in human-machine interface (HMI) control panel. To determine the best conditions to concentrate the cranberry juice *via* RO, a model solution containing glucose and citric acid was used as the feed material due to the high-volume requirement of the pilot unit. Glucose and citric acid are the main sugar and organic acid present in cranberry juice, respectively.<sup>40</sup> The model solution was prepared by dissolving glucose powder (TLC Ingredients, Inc., Crest Hill, IL, USA) in deionized water until the total soluble solids content (TSSC) was  $7.6 \pm 0.2$ ° Brix (~Brix for commercial cranberry juice). The pH of the model solution was adjusted to 2.5 using anhydrous citric acid (ADM, Decatur, IL, USA) to match the pH of single-strength cranberry juice. During RO concentration, the transmembrane pressure was varied: 2.5, 3.0, and 3.5 MPa. After the best condition was determined from the model solution RO experiments, it was used to concentrate the pasteurized, single-strength cranberry juice (5.5° Brix, pH 2.6) sourced from Ocean Spray Cranberries, Inc. (Middleborough, MA, USA).

A similar RO procedure was applied to both glucose solution and cranberry juice. A total of 150 kg of model solution or juice were loaded into the feed tank. Then, the feed was pumped into a heat exchanger to achieve the target processing temperature of 25 °C. The feed passed through the two booster pumps used to achieve the desired TMP and then to the membrane. The retentate was recirculated to the system until the end of the processing. The permeate was collected separately in stainless steel buckets. The RO process was ended when the permeate flow rate was negligible to none. The RO concentrate was collected for analysis and stored at 4 °C until FO processing.

To ensure membrane performance, CIP cleaning was conducted after each run following the recommendation of the



## (a) Reverse Osmosis



## (b) Forward Osmosis

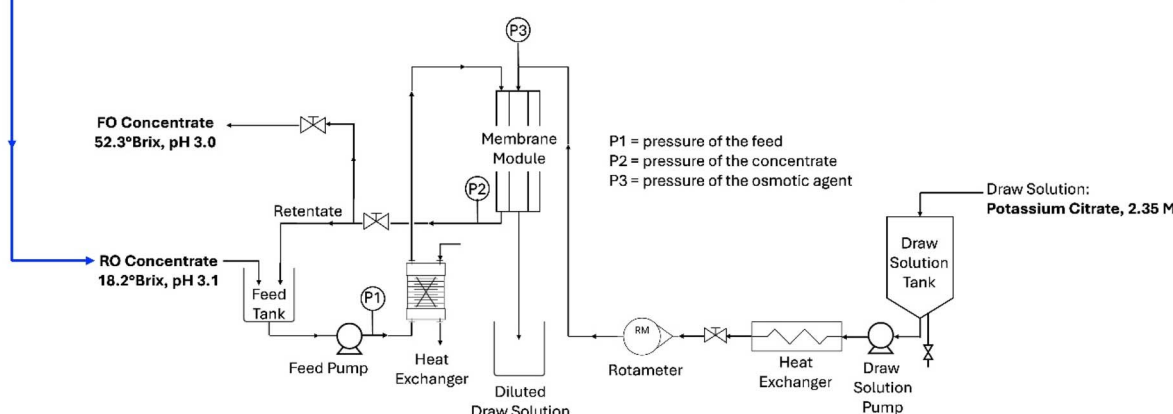


Fig. 1 Schematic diagram of (a) reverse osmosis<sup>46</sup> and (b) forward osmosis concentration processes.

manufacturer. The cleaning was conducted at a TMP of 4 MPa. The unit was rinsed with deionized water to remove the product residue. Afterwards, alkaline cleaning was performed using Ultrasil 110 (Ecolab, Saint Paul, MN) mixed with deionized water at pH 10.5–11.0. The alkaline solution was recirculated in the unit for 30 min at 46–48 °C. The solution was drained and the unit was rinsed with deionized water until pH recovery on the permeate side. An enzymatic cleaning followed. A solution of Ultrasil 110 was prepared following the procedure for alkaline cleaning except that the pH was between 9.75 and 10.5. After recirculating the Ultrasil 110 solution in the unit for 2 min at 46–48 °C, Ultrasil 67 (Ecolab, Saint Paul, MN) was added at 0.4% (v/v) and recirculated for 28 min. The solution was drained and the unit was rinsed with deionized water until pH recovery on the permeate side. Acid cleaning followed by mixing Ultrasil 75 (Ecolab, Saint Paul, MN) in deionized water to achieve a pH of 2.0–3.0. The acid solution was recirculated in the unit for

30 min at 38 °C. After acid cleaning, the solution was drained and the unit was rinsed with deionized water until pH recovery on the permeate side. Water flux was measured after cleaning to evaluate the efficiency. The membrane was stored in 0.5% sodium metabisulfite solution during storage to prevent microbial growth.

The fouling mechanism during the RO concentration of cranberry juice was determined using Hermia's filtration models reported in Brown *et al.* (2008)<sup>41</sup> and Quoc *et al.* (2022),<sup>42</sup> which include complete blocking filtration, intermediate blocking filtration, standard blocking filtration, and cake layer formation. The assumptions, descriptions and linearized form of the equations of each fouling mechanism have been previously described by Brown *et al.* (2008)<sup>41</sup> and Garcia-Castello *et al.* (2011).<sup>43</sup> The RO permeate flux data and time were fitted in the linearized form of each filtration model and linear regression was performed to determine the best fit.



## 2.2 Forward osmosis (FO) concentration

The FO membrane used had a pH operating limit of 3–8 feed pH. Thus, before FO concentration, the pH of the draw solution and the RO-concentrated cranberry juice were adjusted. For the RO-concentrated juice, the pH was increased from 2.4 to  $3.1 \pm 0.1$  by adding potassium bicarbonate (Chem-Impex International, Wood Dale, IL, USA). Food-grade potassium citrate was used as the draw solution (DS) to match the cranberry juice composition with citric acid as the predominant organic acid and potassium as the main mineral.<sup>40</sup> The DS was prepared by dissolving potassium citrate (ADM, Decatur, IL, USA) in deionized water to a concentration of  $2.35 \text{ mol L}^{-1}$ , providing an osmotic pressure of 35 MPa. Then, the pH was decreased from 8.3 to 7.0 using anhydrous citric acid (Alpha Chemicals, Cape Girardeau, MO, USA).

The FO concentration was done using the evapEOS® micro pilot unit (Ederna SAS, Toulouse, France) and the schematic diagram is shown in Fig. 1b. The unit was equipped with a cellulose triacetate spiral-wound membrane (Fluid Technology Solutions, Inc., Albany, OR, USA) with an effective filtration area of  $0.54 \text{ m}^2$ . The membrane has a draw solution sugar rejection rate of 99.9%. During FO concentration, 10 L of cranberry juice was transferred into the feed tank as the initial volume. The juice was pumped into a heat exchanger at an initial feed pressure of 0.1 MPa and then passed on the active layer side of the membrane (AL-FS mode). The retentate was returned to the feed tank and recirculated until the end of processing. Similarly, the draw solution was pumped at a rate of  $7.6 \text{ kg h}^{-1}$  to a heat exchanger and then passed on the support layer side of the membrane in a co-current flow. The diluted draw solution was collected and was not recirculated into the system. Both the feed and the draw solution were maintained at  $25^\circ \text{C}$ . The FO process was ended when the difference in pressure between the feed and the concentrate reached 70 kPa, the operational limit of the membrane.<sup>44</sup> The RO + FO concentrated cranberry juice was collected, packaged in 50 mL polypropylene bottles and stored refrigerated at  $4 \pm 1^\circ \text{C}$  until further analysis.

After juice concentration, the membrane was cleaned following the procedure reported by Beldie *et al.* (2025).<sup>45</sup> Briefly, the cleaning procedure includes enzymatic alkaline cleaning, acid cleaning and disinfection. Rinsing with deionized water was performed between each cleaning step. The water flux was measured after cleaning steps to ensure that membrane performance is maintained.

## 2.3 Shelf life study and analysis of cranberry juice

Refrigerated shelf-life study was conducted for 6 months with 1 month sampling interval on concentrated and reconstituted RO + FO juice. The reconstituted juice was prepared by adding deionized water to the concentrate until the TSSC was  $5.5^\circ \text{ Brix}$ . The single-strength cranberry juice (before RO), the RO concentrate, the RO reconstituted juice, the FO concentrate and the FO reconstituted juices were analyzed to determine the effects of processing on juice quality. The reconstituted juice samples were prepared on the same day before conducting the analysis.

**2.3.1 Physicochemical analyses.** The TSSC (as  $^\circ \text{Brix}$ ) was measured using a digital refractometer (300053, Sper Scientific, Scottsdale, AZ, USA). The pH was measured using the Orion™ Versa Star Pro™ Benchtop pH Meter (Thermo Fisher Scientific, Waltham, MA, USA). The water activity ( $a_w$ ) was measured using the AQUALAB 4TE meter (Meter Group, Pullman, WA, USA).

The titratable acidity was measured by potentiometric titration according to AOAC method (942.15, 2019) with modifications.<sup>47</sup> A 10 mL aliquot of reconstituted cranberry juice concentrate was titrated with  $0.1 \text{ mol L}^{-1}$  NaOH (Ricca, Arlington, TX, USA) using EasyPlus Automated Titrator (Mettler Toledo, LLC, Columbus, OH, USA) until the endpoint pH of 8.2. The results were expressed as anhydrous citric acid ( $\text{g L}^{-1}$ ) and calculated as follows:

$$\text{Titratable acidity} = (V_{\text{NaOH}} \times 0.1 \times 64) / V_{\text{sample}} \quad (1)$$

where  $V$  is the volume of NaOH or the sample in mL, 0.1 is the molarity ( $\text{mol L}^{-1}$ ) of NaOH, and 64 is the anhydrous citric equivalence factor ( $\text{g mol}^{-1}$ ).

Citric and malic acids were quantified using enzymatic assays at the Cornell Craft Beverage Analytical Lab, Cornell AgriTech, Geneva, NY. Samples were prepared, and citric and malic acids were quantified following the procedure in citrate lyase/malate dehydrogenase and L-malate dehydrogenase kits (BioSystems, Costa Brava, Barcelona, Spain), respectively. The absorbances of the test solutions were read at 340 nm in a photometer (SPICA, BioSystems, Costa Brava, Barcelona, Spain). Deionized water was used as a blank and the results were reported as  $\text{g L}^{-1}$ .

The color was measured using UltraScan VIS colorimeter (HunterLab, Reston, Virginia, USA) equipped with D65/10° illuminant-observer combination. The sample was transferred to a cuvette with 1 cm pathlength and measured in the colorimeter using total transmission mode. The CIE  $L^*$ ,  $a^*$ , and  $b^*$  values were recorded and the total color difference ( $\Delta E$ ) was calculated as follows:

$$\Delta E = \sqrt{(\Delta L^*)^2 + (\Delta a^*)^2 + (\Delta b^*)^2} \quad (2)$$

The percent polymeric color (PPC) was determined using the bisulfite method according to Dorris *et al.* (2018)<sup>48</sup> with modifications. Juice samples were diluted 20-fold using deionized water. Two cuvettes were prepared and 2.8 mL of diluted juice sample were transferred in each. Then, 0.2 mL of deionized water was added to one of the cuvettes and 0.2 mL of bisulfite solution ( $0.2 \text{ mg mL}^{-1}$ ) to the other. The mixtures were equilibrated for 15 min before measurement. The absorbance ( $A$ ) of each cuvette was read in a UV-Vis spectrophotometer (GENESYS 20, Thermo Spectronic, Rochester, NY, USA) at 420, 520, and 700 nm wavelengths. PPC was calculated using the eqn (3) below:

$$\% \text{ Polymeric color (PPC)} = \frac{\text{polymeric color}}{\text{color density}} \times 100 \quad (3)$$

where polymeric color (bisulfite bleached sample) was calculated as



$$\text{Polymeric color (PC)} = [(A_{420} - A_{700}) + (A_{520} - A_{700})] \times \text{DF} \quad (4)$$

and DF was the dilution factor. The color density (sample with water) was calculated as

$$\text{Color density} = [(A_{420} - A_{700}) + (A_{520} - A_{700})] \times \text{DF} \quad (5)$$

The turbidity was measured by transferring 10 mL of juice into the sample tube and was read using a turbidity meter (2020wi, LaMotte, Chestertown, MD, USA). The results were reported as Formazin Nephelometric Units (FNU).

**2.3.2 Phenolics and antioxidant activity analyses.** The total phenolic content (TP) was determined following the Folin-Ciocalteau colorimetry microscale protocol.<sup>49</sup> A 20-fold dilution of the reconstituted cranberry juice concentrate was prepared as the test sample. The absorbance was read at 765 nm wavelength using a UV-Vis spectrophotometer (GENESYS 20). The TP was calculated against a gallic acid (Chem-Impex Int'l, Wood Dale, IL, USA) calibration curve and expressed as gallic acid equivalent (mg GAE per L).

The total monomeric anthocyanin (TMA) was determined according to Lee *et al.* (2005).<sup>50</sup> Juice samples were diluted 20-fold with potassium chloride buffer (0.025 mol L<sup>-1</sup>, pH 1.0) and sodium acetate buffer (0.4 mol L<sup>-1</sup>, pH 4.5) and allowed to equilibrate for 15 min. The absorbance of the diluted samples was read at 520 and 700 nm wavelengths in a UV-Vis spectrophotometer using a cuvette with 1 cm pathlength. Distilled water was used as a blank. The TMA was calculated using eqn (6) and the results were expressed as cyanidin-3-glucoside equivalent (mg CGE per L).

$$\text{TMA} = \frac{A \times \text{MW} \times \text{DF} \times 1000}{\varepsilon \times 1} \quad (6)$$

where  $A = (A_{520} - A_{700})_{\text{pH } 1.0} - (A_{520} - A_{700})_{\text{pH } 4.5}$ ;  $A_{520}$  and  $A_{700}$  are the absorbance readings from the spectrophotometer at 520 nm and 700 nm wavelengths, respectively; MW = 449.2 g mol<sup>-1</sup>; DF is the dilution factor; and  $\varepsilon = 26\,900 \text{ L} \times \text{mol}^{-1} \times \text{cm}^{-1}$ .

The total flavonoid content (TF) was determined according to Nowak *et al.* (2022).<sup>51</sup> Juice samples were diluted 20-fold with deionized water. Then, 1 mL of diluted juice sample was pipetted to a test tube and 0.3 mL of 5% sodium nitrate solution was added and vortexed briefly. The mixture was left to stand for 5 min. Afterward, 0.3 mL of 10% aluminum chloride solution was added, vortexed briefly, and left to stand. After 1 min, 2 mL of 1 mol L<sup>-1</sup> NaOH solution and 2.4 mL of deionized water were added and vortexed briefly. The mixture was transferred to a 1 cm plastic cuvette and the absorbance was measured in a UV-Vis spectrophotometer at 510 nm wavelength. The TF was determined by plotting the absorbance against a quercetin (Sigma Chemical, St. Louis, MO, USA) standard curve. The values are expressed as quercetin equivalent (mg QE per L).

Antioxidant activities were determined using DPPH and ABTS assays. DPPH assay was conducted according to Nowak *et al.* (2022).<sup>51</sup> The DPPH (TCI America, Portland, OR, USA) was dissolved in methanol to a concentration of 0.1 mmol L<sup>-1</sup> and the absorbance was adjusted to 1.00 ± 0.05 before using. Single-strength and reconstituted juice samples were diluted 20-fold

with deionized water. A 0.1 mL of diluted juice was added to 2.9 mL 0.1 mmol L<sup>-1</sup> DPPH solution and mixed. The mixture was incubated for 30 min in the dark at room temperature. Then, the absorbance of the mixture was measured in a 1 cm cuvette at 517 nm using a UV-Vis spectrophotometer. The ABTS assay was performed according to Re *et al.* (1999)<sup>52</sup> with modifications. A 7 mmol L<sup>-1</sup> ABTS stock solution was prepared by dissolving ABTS (Sigma-Aldrich, St. Louis, MO, USA) salt in deionized water. Then, potassium persulfate (Honeywell, Muskegon, MI, USA) was added in the ABTS stock solution to a final concentration of 2.45 mmol L<sup>-1</sup>. The mixture was stored in the dark at room temperature for 12–16 h. The absorbance of the ABTS-potassium persulfate solution was adjusted to 0.70 ± 0.02 at 734 nm using methanol before analysis. Single-strength and reconstituted juice samples were diluted 10-fold with deionized water. A 20 µL of juice samples were mixed with 2 mL ABTS-persulfate solution and left to stand for 6 min in the dark at room temperature. Then, the absorbance was read in a cuvette with 1 cm pathlength using a UV-Vis spectrophotometer at 734 nm wavelength. The resulting absorbance for DPPH and ABTS was plotted against a Trolox (AG Scientific, San Diego, CA, USA) calibration curve and the results were reported as Trolox equivalent (mg TE per L).

## 2.4 Kinetic data calculation for TMA degradation and PC formation

The kinetics of total monomeric anthocyanins (TMA) degradation and polymeric color (PC) formation in cranberry juice during refrigerated storage for 6 months were estimated using zero-order (eqn (7)) and first-order (eqn (8)) kinetic models:<sup>53</sup>

Zero-order:

$$C_t = C_0 - k_0 t, \quad t_{1/2} = C_0 / 2k_0 \quad (7)$$

First-order:

$$\ln(C/C_0) = -k_1 t, \quad t_{1/2} = -\ln 0.5 / k_1 \quad (8)$$

where  $C_0$  and  $C_t$  are the concentration (mg CGE per L for TMA and Absorbance Units for PC) at time 0 and at any time  $t$ , respectively,  $k_0$  is the zero-order constant (units/month),  $k_1$  is the first-order rate constant (per month),  $t$  and  $t_{1/2}$  are the time and half-life in months of refrigerated storage.

## 2.5 Microbiological analyses

The cranberry juice concentrates before FO, after FO, and during 1, 3 and 6 months of refrigerated storage were analyzed for total plate count (TPC) and yeast and mold count (Y&M). The samples were analyzed at the Microbial Food Extension Lab at Cornell AgriTech, Geneva, NY. Briefly, for TPC, 1 mL of concentrated juice was serially diluted with 0.1% peptone water (Difco, Becton Dickinson, Sparks, MD, USA). Then the mixture was pour-plated in plate count agar (Alpha Biosciences, Baltimore, MD, USA) and incubated at 30 °C for 48 to 72 h. For Y&M, the same procedure was performed, except that the diluted samples were transferred to plates with potato dextrose agar (Alpha Biosciences, Baltimore, MD, USA) adjusted to pH 3.5.



with tartaric acid (Sigma Chemical Co., St. Louis, MO, USA). Microbiological analyses were conducted in triplicates and each sample was plated in duplicates.

## 2.6 Statistical analysis

All trials were performed in triplicate. Data were analyzed with one-way ANOVA with Tukey's HSD *post-hoc* test to determine significance. The difference was deemed statistically significant at  $p < 0.05$ . Spearman's correlation was used to determine the correlation coefficients between variables. All analyses were done using JMP Pro 17 statistical software (JMP Statistical Discovery LLC, Cary, NC, USA).

## 3 Results and discussion

### 3.1 Reverse osmosis concentration of model solution

During reverse osmosis (RO) concentration of the model solution, the transmembrane pressure (TMP) directly influenced the permeate water flux (see Fig. 2), where flux increased when the TMP was higher. This observation is typical of the RO process<sup>54,55</sup> due to increased driving force when operating at higher TMP.<sup>23,56</sup> As mentioned earlier, RO with TMP of up to 7.0 MPa was used to concentrate juices but this study limited the maximum TMP to 3.5 MPa to be within the recommended typical membrane operating pressure of 1.5–4.0 MPa. Although further increasing the TMP could result in higher fluxes, at higher TMP, a limiting flux can be encountered where flux no longer increases when pressure is increased.<sup>57</sup> This observation was reported by Menchik & Moraru (2019)<sup>58</sup> during RO concentration of acid whey where a plateau in flux was reached at TMP higher than 3.5 MPa and could be a result of membrane compaction at higher pressure, thereby limiting water permeability.<sup>59</sup> At the end of RO concentration of the model solution, the total soluble solids content (TSSC) achieved at TMP of 2.5, 3.0 and 3.5 MPa were  $14.1 \pm 0.2$ ,  $16.6 \pm 0.2$  and  $18.1 \pm 0.4$ ° Brix

respectively. From these results, the RO concentration of cranberry juice was carried out at a TMP of 3.5 MPa.

### 3.2 Reverse osmosis and forward osmosis concentration of cranberry juice

The RO permeate flux during cranberry juice concentration behaved similarly to the permeate flux of the model solution at 3.5 TMP (see Fig. 2). When compared to FO concentration, RO had a higher water flux at the beginning of the process than FO as shown in Fig. 3, due to the higher effective pressure differential brought about by the external pressure applied in RO.<sup>60</sup> However, RO has a rapid and steep decline in flux compared to FO. The results of the statistical evaluation of Hermia's fouling mechanism models (see Table 1) showed that complete blocking best fitted the model. Since the correlation coefficients between complete blocking, standard blocking, and intermediate blocking differ by <10%,<sup>41</sup> it can be inferred that the RO runs exhibited these mechanisms. The decline in flux during RO concentration of cranberry juice could primarily be due to the combined effects of fouling, resulting from multiple pore-blocking mechanisms occurring simultaneously, and concentration polarization, resulting from the increase in osmotic pressure brought by the increase in TSSC.<sup>42,61</sup>

On the other hand, during FO concentration using asymmetric membranes, the permeate flux decline was slower and predominantly caused by internal concentration polarization<sup>62</sup> due to the increase in osmotic pressure of the feed as the concentration proceeds. Other factors can contribute to FO flux decline, such as the juice composition, which can result in fouling of the membrane.<sup>29,63</sup> During the FO concentration of grapefruit juice, unfiltered juice caused a rapid flux decline compared to the filtered juice due to the presence of the pulp, suspended solids and pectin.<sup>64</sup> In this study, the cranberry juice was clarified prior to the concentration steps, thus, the reduction in the flux as concentration progresses during FO can be

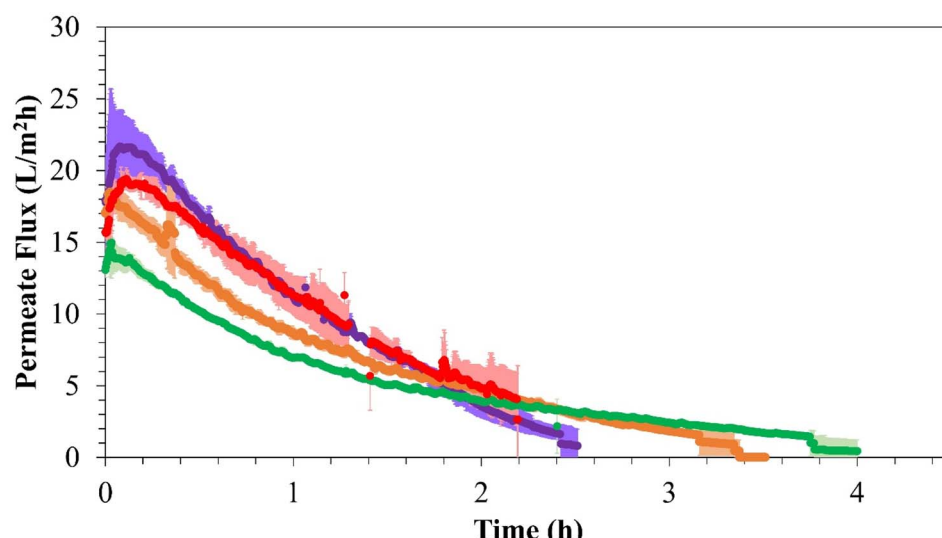


Fig. 2 Permeate fluxes during reverse osmosis concentration of model solution at transmembrane pressures of (●) 2.5, (○) 3.0, and (●) 3.5 MPa, and (●) cranberry juice at 3.5 MPa. Values presented are mean  $\pm$  standard deviation.



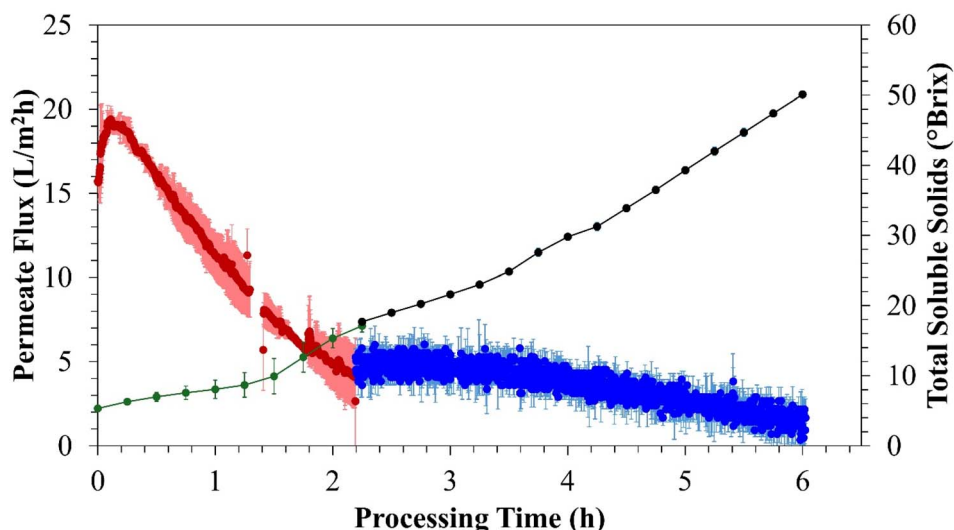


Fig. 3 Permeate flux and total soluble solids content (TSSC) during reverse osmosis (RO) and forward osmosis concentration of cranberry juice. Values presented are mean  $\pm$  standard deviation. (●) RO flux; (●) FO flux; (●) TSSC during RO; (●) TSSC during FO.

Table 1 Statistical results of Hermia's fouling mechanism models for reverse osmosis process<sup>a</sup>

Fouling mechanism	R <sup>2</sup>	RMSE
Complete blocking	0.986	0.056
Standard blocking	0.960	0.016
Intermediate blocking	0.913	0.017
Cake layer formation	0.751	0.008

<sup>a</sup> R<sup>2</sup> = correlation coefficient; RMSE = root mean square error.

attributed to the increase in the TSSC, causing a reduction in the osmotic pressure gradient between the juice and the draw solution.<sup>35,65,66</sup> Similarly, the increase in juice viscosity as a result of an increased TSSC can exacerbate concentration polarization and can increase the resistance of the water to flow through the membrane, therefore reducing the permeate flux.<sup>67,68</sup> To better understand the fouling mechanisms both in RO and FO processes, a microscopic analysis, such as SEM, of the membrane would be beneficial to include in further studies.

Fouling phenomena occurs in RO and FO processes and coupling with other technologies can address fouling and other

challenges with membrane processing. Both electric field and ultrasound was applied to membrane processes to mitigate fouling. In the studies of Jiang *et al.* (2019)<sup>69</sup> and Rouina *et al.* (2016),<sup>70</sup> the electromagnetic field-assisted RO resulted in an increased membrane performance and controlled membrane fouling and scaling. In a study by Trishitman (2025)<sup>71</sup> on FO concentration of pomegranate juice, the ultrasound-assisted FO enhances the flux performance by reducing fouling and mitigating concentration polarization. While improvement was observed in FO performance and concentration time with ultrasound, it was accompanied by an increase in reverse solute diffusion. A similar observation was reported in several studies on ultrasound-assisted forward osmosis.<sup>72,73</sup> Although the effect on process performance was illustrated, it poses a challenge in terms of the scalability of the assisted membrane process.

After RO concentration, the TSSC of cranberry juice was  $17.80 \pm 0.04$ ° Brix as shown in Table 2. After further concentrating by FO, the TSSC of cranberry juice was  $52.3 \pm 0.7$ ° Brix (see Table 2). With the combined processes, cranberry juice was concentrated to 3.2-fold using RO and to 9.5-fold after FO from an initial TSSC of 5.5° Brix. The TSSC level achieved was still below the typical range of thermal concentrate ( $\sim 67$ –70° Brix)

Table 2 Selected physicochemical properties of cranberry juice concentrate before RO, after RO and after FO processing<sup>a</sup>

	Before RO	RO concentrate	FO concentrate
Total soluble solids, °Brix	$5.50 \pm 0.01$	$17.80 \pm 0.04$	$52.3 \pm 0.7$ <sup>a</sup>
pH	$2.56 \pm 0.01$	$2.40 \pm 0.01$	$3.02 \pm 0.05$ <sup>a</sup>
<i>a</i> <sub>w</sub>	$0.991 \pm 0.001$	$0.979 \pm 0.001$	$0.893 \pm 0.003$
<b>Color</b>			
<i>L</i> <sup>*</sup>	$40.3 \pm 0.1$	$21.8 \pm 0.2$	$5.5 \pm 0.2$
<i>a</i> <sup>*</sup>	$69.5 \pm 0.1$	$56.4 \pm 0.3$	$32.2 \pm 0.4$
<i>b</i> <sup>*</sup>	$53.6 \pm 0.4$	$36.9 \pm 0.3$	$8.9 \pm 0.6$

<sup>a</sup> pH raised by K<sub>2</sub>CO<sub>3</sub> addition due to FO membrane pH limitation.



due to the limitations of the equipment impeding higher TSSC but the process still offers benefits on transport and storage costs due to the significant volume reduction while retaining juice quality. This study used a benchtop FO unit where the process needed to stop due to the pressure operational limitations of the equipment, *i.e.* when the difference in pressure between the feed and the concentrate reached 70 kPa.<sup>44</sup> However, this limitation can be easily overcome in a different membrane system such as the continuous industrial-scale FO system which was demonstrated to concentrate watermelon juice by FO to  $\sim$ 65° Brix in a study by Milczarek *et al.* (2020).<sup>74</sup>

The RO and FO process has potential industrial implications in terms of energy consumption, cost and environmental impacts. It was shown that up to 90% reduction in energy consumption and up to 85% reduction in energy cost can be achieved during RO concentration of maple syrup, compared to thermal evaporation.<sup>75</sup> FO is also less energy-intensive, providing up to 80% in energy savings and up to 94% lower greenhouse emissions compared to thermal concentration, while retaining juice quality.<sup>76</sup> Large-scale RO units exist especially with RO application in wastewater treatment. For FO, although the use of an industrial scale was demonstrated,<sup>74</sup> the process was still accompanied by several challenges such as internal concentration polarization, reverse solute flux and regeneration of the draw solution which can be energy intensive.<sup>77</sup> These challenges require further membrane development and identification of draw solutions that will provide high permeate water flux, low reverse solute flux and can easily be regenerated.<sup>78</sup>

Freeze concentration is another nonthermal concentration process used for juices can produce a product that is very similar to the original juice. It can be advantageous over membrane separation processes like reverse osmosis and forward osmosis, which can prevent nutrient losses due to permeation. However, it requires freezing which can be energy-intensive and costlier in terms of capital and operational expenses.<sup>11,79</sup> Freeze concentration can be slower and a challenge for high-volume production. Lastly, the achievable total soluble content may be limited compared to forward osmosis concentration.<sup>11</sup>

### 3.3 Physicochemical and antioxidant properties of cranberry juice before and after RO and FO processing

The juice concentrates after processing were reconstituted to the original TSSC and then analyzed to determine the effect of RO and FO processing. The reconstituted samples were compared to the juice before RO and the results for different juice properties are shown in Table 3. There were no significant changes ( $p > 0.05$ ) in pH and titratable acidity before and after RO and before and after FO. The difference in pH and titratable acidity of the reconstituted juice after RO and before FO was mainly due to the addition of potassium bicarbonate to adjust the pH before FO and was not an effect of the process. The adjustment was necessary due to the limitations of the operating pH range (3–8) of the FO membrane.

A small reduction (4%) in total monomeric anthocyanin content from  $66.4 \pm 0.7 \text{ mg L}^{-1}$  to  $63.8 \pm 0.6 \text{ mg L}^{-1}$  was observed after RO concentration but remained the same after

**Table 3** Physicochemical properties of cranberry juice samples, as single strength, before and after reverse osmosis (RO) and forward osmosis (FO)<sup>a</sup>

	Before RO	RO conc. recon.	Before FO recon.	FO conc. recon.
Total soluble solids content, °Brix	$5.50 \pm 0.01$	$5.50 \pm 0.01$	$5.50 \pm 0.01$	$5.50 \pm 0.01$
pH	$2.56 \pm 0.01^a$	$2.54 \pm 0.01^a$	$3.05 \pm 0.03^b$	$3.04 \pm 0.06^b$
$a_w$	$0.991 \pm 0.001$	$0.993 \pm 0.001$	$0.993 \pm 0.000$	$0.993 \pm 0.001$
Titratable acidity, g L <sup>-1</sup>	$15.92 \pm 0.35^a$	$15.84 \pm 0.07^a$	$13.89 \pm 0.10^b$	$13.72 \pm 0.20^b$
Citric acid, g L <sup>-1</sup>	$7.70 \pm 0.06^a$	$7.49 \pm 0.20^a$	$7.54 \pm 0.07^a$	$7.49 \pm 0.21^a$
Malic acid, g L <sup>-1</sup>	$5.06 \pm 0.08^a$	$4.86 \pm 0.04^{bc}$	$4.95 \pm 0.04^{ab}$	$4.70 \pm 0.07^c$
<b>Color</b>				
$L^*$	$40.3 \pm 0.1^a$	$40.0 \pm 0.5^{ab}$	$39.1 \pm 0.2^b$	$39.0 \pm 0.7^b$
$a^*$	$69.5 \pm 0.1^a$	$67.6 \pm 1.3^b$	$67.1 \pm 0.2^b$	$66.5 \pm 0.1^b$
$b^*$	$53.6 \pm 0.4^a$	$50.9 \pm 3.5^{ab}$	$46.8 \pm 1.0^b$	$46.6 \pm 2.2^b$
$\Delta E$	—	$3.3 \pm 0.0$	$7.3 \pm 0.9$	$7.8 \pm 2.0$
% polymeric color	$17.6 \pm 1.6^a$	$18.1 \pm 1.0^b$	$24.7 \pm 2.4^b$	$20.0 \pm 3.6^{ab}$
Total phenolics content, mg GAE per L	$1190 \pm 190^a$	$1300 \pm 200^a$	$1415 \pm 98^a$	$1318 \pm 97^a$
Total monomeric anthocyanin, mg CGE per L	$66.4 \pm 0.7^a$	$63.8 \pm 0.6^b$	$62.8 \pm 1.0^b$	$62.5 \pm 0.6^b$
Total flavonoid content, mg QE per L	$1306 \pm 21^a$	$1307 \pm 44^a$	$1355 \pm 52^a$	$1345 \pm 60^a$
<b>Antioxidant activity</b>				
DPPH, mg TE per L	$1998 \pm 51^a$	$1460 \pm 170^b$	$1860 \pm 140^a$	$1770 \pm 150^a$
ABTS, mg TE per L	$2860 \pm 130^a$	$2530 \pm 360^a$	$2865 \pm 66^a$	$2900 \pm 200^a$

<sup>a</sup> RO conc. recon. – reconstituted RO concentrate; before FO recon. – reconstituted RO concentrate after pH adjustment; FO conc. recon – reconstituted FO concentrate. GAE – gallic acid equivalent; CGE – cyanidin-3-glucoside equivalent; QE – quercetin equivalent; TE – trolox equivalent. The titratable acidity is expressed as anhydrous citric acid. Values presented are mean  $\pm$  standard deviation ( $n = 3$ ). Values with different letters in each row are significantly different (ANOVA, Tukey's HSD,  $p < 0.05$ ).



Table 4 Selected physicochemical properties of cranberry juice RO + FO concentrate during refrigerated storage<sup>a</sup>

Color	Storage, months						
	0	1	2	3	4	5	6
$L^*$	5.5 ± 0.2 <sup>a</sup>	5.6 ± 0.2 <sup>a</sup>	5.3 ± 0.5 <sup>a</sup>	4.7 ± 0.3 <sup>ab</sup>	4.2 ± 0.4 <sup>bc</sup>	3.8 ± 0.2 <sup>c</sup>	3.5 ± 0.2 <sup>c</sup>
$a^*$	32.2 ± 0.4 <sup>a</sup>	32.7 ± 0.7 <sup>a</sup>	30.4 ± 0.9 <sup>ab</sup>	29.1 ± 0.8 <sup>bc</sup>	27.0 ± 1.4 <sup>cd</sup>	24.5 ± 1.2 <sup>de</sup>	22.6 ± 1.4 <sup>e</sup>
$b^*$	8.9 ± 0.6 <sup>a</sup>	9.1 ± 0.0 <sup>a</sup>	8.5 ± 0.2 <sup>a</sup>	7.4 ± 0.5 <sup>b</sup>	6.6 ± 0.1 <sup>bc</sup>	6.0 ± 0.3 <sup>cd</sup>	5.5 ± 0.5 <sup>d</sup>
$\Delta E$	—	0.7 ± 0.2	2.0 ± 0.6	3.5 ± 0.4	5.9 ± 0.7	8.4 ± 0.6	10.4 ± 0.9

<sup>a</sup> Values are mean ± standard deviation ( $n = 3$ ). Values with different letters in each row are significantly different (ANOVA, Tukey's HSD,  $p < 0.05$ ).

FO concentration. Several studies reported that the reduction in the TMA levels can be attributed to several factors such as the presence of oxygen and enzymes during the processing<sup>80,81</sup> or some could be lost to the permeate.<sup>82,83</sup> In the case of our experimental runs, an equivalent of  $0.7 \pm 0.1$  mg CGE per L of TMA was quantified in the RO permeate, suggesting losses of TMA to the RO permeate. A similar observation was reported where anthocyanins were lost to the permeate during RO concentration of grape juice.<sup>84</sup> There were no significant

changes in the total phenolics content and total flavonoid content before and after RO and FO processing, as shown in Table 3, indicating the positive effect of the nonthermal processes on retaining polyphenolic compounds.

Changes in color were observed after RO and FO processing as indicated by  $\Delta E$  increase when the reconstituted samples were compared to the original juice as shown in Table 3. Choi *et al.*<sup>85</sup> and Cserhalmi *et al.*<sup>86</sup> indicated that a  $\Delta E \geq 2.0$  can be visible when samples are compared side by side. When the pH

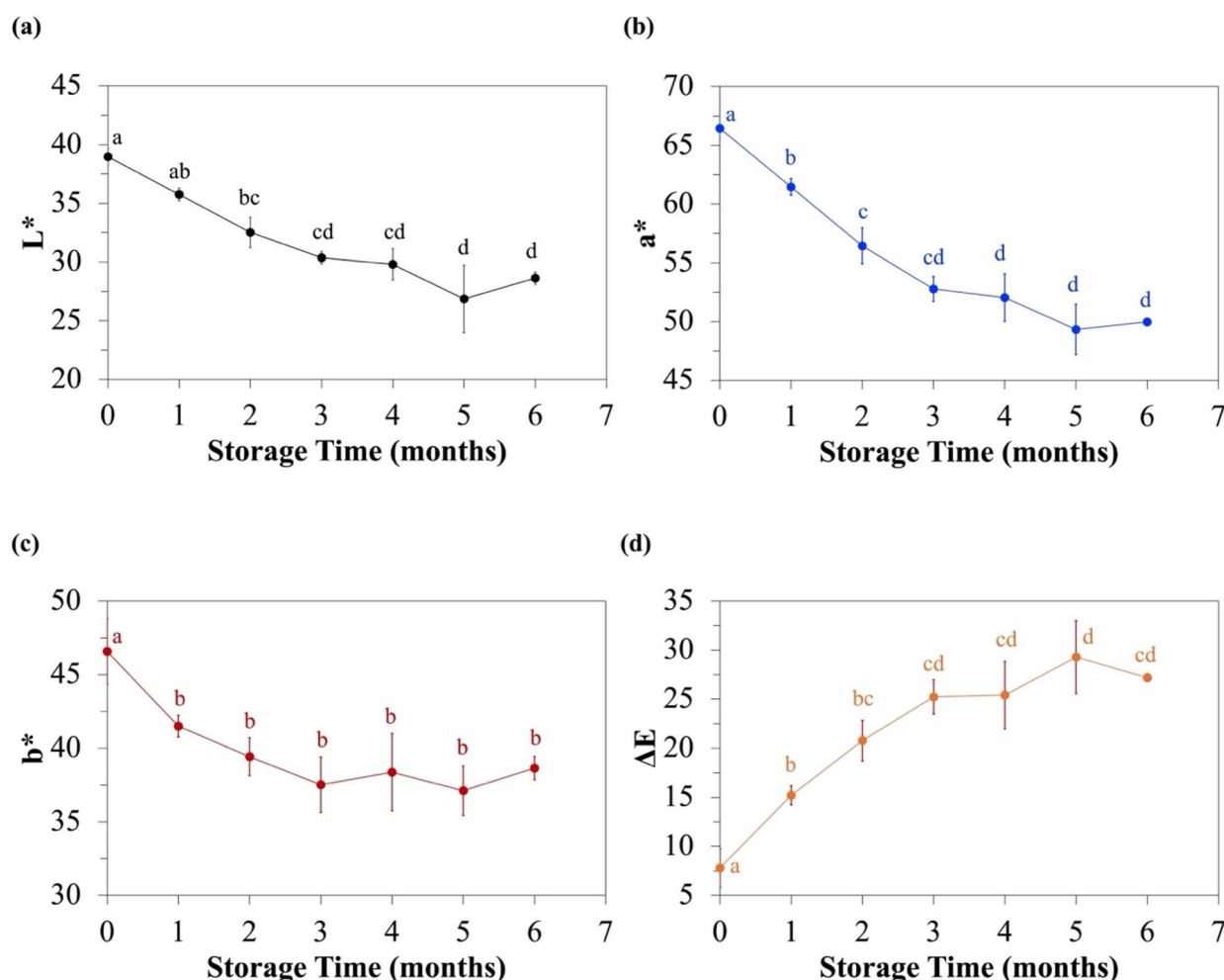


Fig. 4 Color values (a)  $L^*$  – light to dark, (b)  $a^*$  – red to green, (c)  $b^*$  – yellow to blue, and (d)  $\Delta E$  – total color change of reconstituted RO + FO cranberry juice concentrate during refrigerated storage. The values presented are mean ± standard deviation ( $n = 3$ ). Different letters indicate significant difference between storage period (ANOVA, Tukey's HSD,  $p < 0.05$ ).



of the juice was increased before FO concentration, a  $\Delta E = 4.5 \pm 0.3$  was observed, suggesting that there was a color change after RO and before FO. This could be attributed to pH adjustment and not to the degradation of anthocyanin since the TMA and % polymeric color were not statistically different ( $p > 0.05$ ). The increase in pH may have shifted the anthocyanin structures consistent with the pH-dependent color changes reported by Torskangerpoll & Andersen (2005).<sup>87</sup> We recommend conducting quantification of the anthocyanin composition to assess the changes in the pigment composition.

### 3.4 Selected physicochemical properties of RO + FO cranberry juice concentrate during refrigerated storage

After RO and FO concentration, samples were stored refrigerated, and analyses were conducted every month. Table 4 shows the selected physicochemical properties of RO + FO cranberry juice concentrate during 6 months of refrigerated storage. There were no significant changes ( $p > 0.05$ ) in TSSC ( $52.1 \pm 0.7$  to  $52.3 \pm 0.8$ ), pH ( $2.9 \pm 0.1$  to  $3.1 \pm 0.1$ ) and  $a_w$  (0.98) during refrigerated storage of the juice concentrate. However, changes in the  $L^*$ ,  $a^*$  and  $b^*$  color values were observed, with  $a^*$  and  $b^*$  values decreasing significantly after 3 months of storage when compared to the concentrate after processing. Further, the  $\Delta E$  values increased during storage. When compared to juice concentrate after processing, a  $\Delta E = 0.7$  in the first month was recorded, showing a minimal change that is not easily perceived by the naked eye. However, after two months of refrigerated storage, the color change was noticeable since the  $\Delta E > 2.0$ . Color changes were more evident in the reconstituted juice samples, which are discussed in the next section.

### 3.5 Physicochemical properties and antioxidant activity of reconstituted RO + FO cranberry juice concentrate during refrigerated storage

The stored RO + FO cranberry juice concentrate was reconstituted ( $5.5^\circ$  Brix) to evaluate changes over time. There were no significant differences ( $p > 0.05$ ) in pH (3.0–3.1), water activity (0.99), titratable acidity ( $13.3\text{--}13.7\text{ g L}^{-1}$ ), and citric acid content ( $7.5\text{--}8.0\text{ g L}^{-1}$ ) after reconstitution. Color parameters,  $L^*$ ,  $a^*$ , and  $b^*$ , decreased over time (see Fig. 4a–c) similar to the color change observations in RO + FO concentrate. The  $\Delta E$  increased (see Fig. 4d) from  $7.8 \pm 2.0$  to  $27.2 \pm 0.4$  during storage when compared to the initial juice color before RO processing. Although  $L^*$  ( $r = -0.92$ ,  $p < 0.001$ ),  $a^*$ , and  $b^*$  ( $r = -0.92$ ,  $p < 0.001$ ) negatively influenced  $\Delta E$ ,  $a^*$  had the highest influence ( $r = -0.98$ ,  $p < 0.001$ ). The positive value on  $a^*$  refers to redness, thus the reduction from  $66.5 \pm 0.1$  to  $50.0 \pm 0.2$  is an indication of the degradation of anthocyanins present in the juice. Several studies have also reported that the decrease in  $a^*$  is attributed to polymerization or degradation of anthocyanins.<sup>31,88,89</sup> Cranberry juice contains polyphenolic compounds that are responsible for its color<sup>90,91</sup> and the color change could also be due to changes in other pigments during storage. Further studies focusing on quantifying the individual polyphenolic compounds in the cranberry juice will help elucidate their contribution to total color change during refrigerated storage.

The total monomeric anthocyanin content (see Fig. 5a) decreased from  $62.5 \pm 0.6$  to  $26.8 \pm 1.7$  mg CGE per L after 6 months, which was predicted earlier from the color indicator,  $a^*$ . The degradation of monomeric anthocyanins can be attributed to several factors, such as interaction with other compounds present in the juice and polymerization

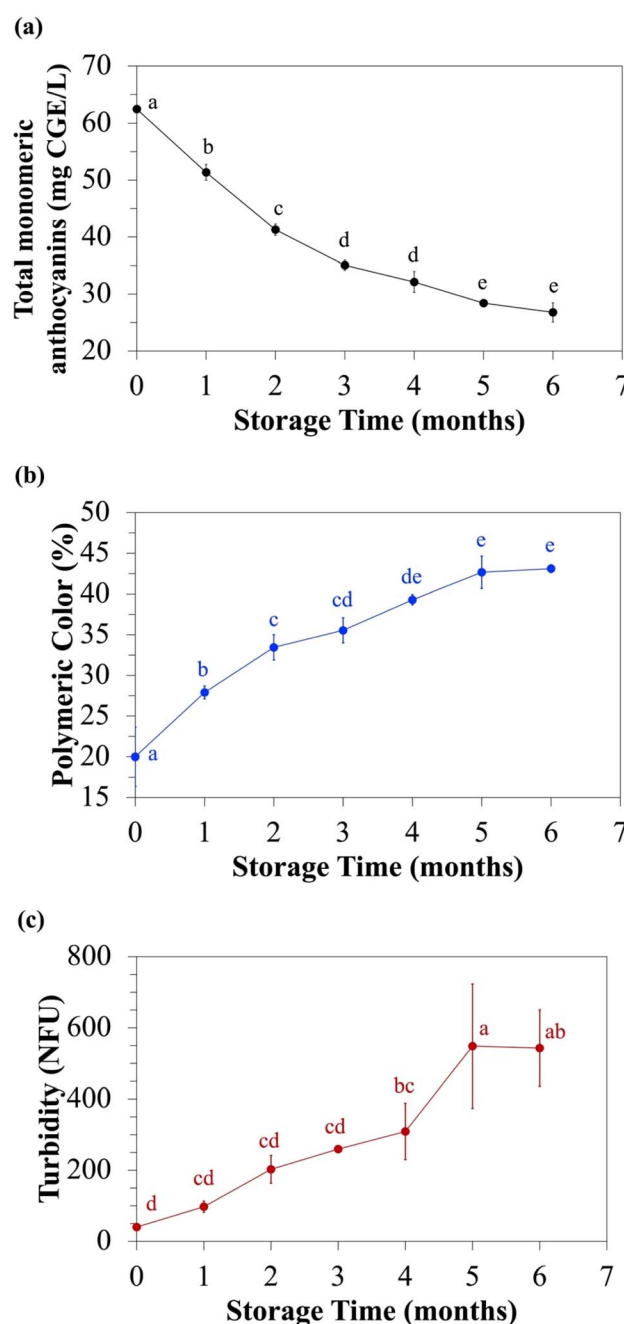


Fig. 5 (a) Total monomeric anthocyanin content, (b) percent polymeric color, and (c) turbidity of reconstituted RO + FO cranberry juice concentrate during refrigerated storage. The values presented are mean  $\pm$  standard deviation ( $n = 3$ ). Different letters indicate significant difference between storage period (ANOVA, Tukey's HSD,  $p < 0.05$ ). CGE = cyanidin-3-glucoside equivalent. NFU = formazin nephelometric units.



Table 5 Physicochemical properties of reconstituted cranberry juice RO + FO concentrate (5.5° Brix) during refrigerated storage<sup>a</sup>

	Storage, month per s							
	0	1	2	3	4	5	6	
Total phenolic content, mg GAE per L	1318 ± 97 <sup>a</sup>	1324 ± 267 <sup>a</sup>	1498 ± 66 <sup>a</sup>	1380 ± 247 <sup>a</sup>	1527 ± 106 <sup>a</sup>	1634 ± 190 <sup>a</sup>	1451 ± 10 <sup>a</sup>	
Total flavonoid content, mg QE per L	1345 ± 60 <sup>a</sup>	1283 ± 95 <sup>a</sup>	1196 ± 134 <sup>a</sup>	1308 ± 136 <sup>a</sup>	1333 ± 48 <sup>a</sup>	1321 ± 51 <sup>a</sup>	1198 ± 92 <sup>a</sup>	
<b>Antioxidant activity</b>								
DPPH, mg TE per L	1769 ± 147 <sup>a</sup>	1645 ± 40 <sup>ab</sup>	1395 ± 255 <sup>ab</sup>	1521 ± 164 <sup>ab</sup>	1496 ± 88 <sup>ab</sup>	1363 ± 58 <sup>b</sup>	1362 ± 88 <sup>b</sup>	
ABTS, mg TE per L	2895 ± 202	2622 ± 524	2414 ± 502	2277 ± 105	2487 ± 143	2322 ± 238	2319 ± 45	

<sup>a</sup> GAE = gallic acid equivalent; CGE = cyanidin-3-glucoside equivalent; QE = quercetin equivalent; TE = trolox equivalent. Values are mean ± standard deviation ( $n = 3$ ) and different letters in each row are significantly different (ANOVA, Tukey's HSD,  $p < 0.05$ ).

reactions.<sup>53,92,93</sup> Percent Polymeric Color (PPC) is another indicator of anthocyanin degradation.<sup>94</sup> When anthocyanins degrade, there is an increase in PPC.<sup>95</sup> The cranberry juice before RO and FO concentration had a PPC of 17.6 ± 1.6 (Table 3). At the end of 6 months, the PPC value (see Fig. 5b) was equal to 43.1 ± 0.5%, more than twice the original, suggesting the polymerization or degradation of anthocyanins during storage. Similar observations occurred during the storage of black carrot juice,<sup>96</sup> strawberry juice,<sup>97</sup> grape juice,<sup>98</sup> and sour cherry juice<sup>99</sup> where PPC increased over time. Similarly, the turbidity followed the same trend as with PPC where it increased during refrigerated storage as shown in Fig. 5c. The turbidity in the cranberry juice was caused by the formation of insoluble complexes that precipitate over time. These precipitates in cranberry juice were the product of anthocyanins being polymerized, mostly consisting of polymeric colors as reported by Dorris & Bolling (2021).<sup>100</sup> To understand the mechanism of degradation, it is suggested that anthocyanins be quantified by other methods. Total phenolic and flavonoid contents had no significant changes ( $p > 0.05$ ) during refrigerated storage as shown in Table 5, further indicating the stability of these compounds when processed by RO and FO.

For antioxidant activities, there were no significant differences ( $p > 0.05$ ) for ABTS values (Table 5). However, a significant reduction (23%) in DPPH was observed during 6 months of refrigerated storage.<sup>100</sup> suggested that anthocyanins in cranberry juice may have more contribution to the antioxidant efficacy compared to the phenolic acids. Although TMA decreased during storage, the DPPH antioxidant activity could not only be attributed to anthocyanins ( $r = 0.67$ ,  $p < 0.001$ ). The overall antioxidant activity may be due to the combined effects of the anthocyanins, phenolics ( $r = -0.56$ ,  $p < 0.01$ ), and flavonoid contents ( $r = 0.55$ ,  $p < 0.01$ ).

### 3.6 Kinetic data for anthocyanin degradation and polymeric color formation

The TMA and polymeric color data were fitted to zero-order and first-order kinetics. The kinetic parameters are shown in Table 6. Linear regression showed that TMA degradation follows a first-order reaction where the reaction rate is proportional to the anthocyanin concentration and indicates that anthocyanin decreases exponentially due to polymerization and

Table 6 Kinetic parameters of anthocyanin degradation and polymeric color formation in reconstituted RO + FO cranberry juice concentrate during refrigerated storage<sup>a</sup>

	Total monomeric anthocyanins	Polymeric color
<b>Zero-order</b>		
$k_0$ , U/months	-5.796	0.130
$R^2$	0.911	<b>0.960</b>
$t_{1/2}$ , months	—	2.8
<b>First-order</b>		
$k_1$ , month per s	-0.142	0.116
$R^2$	<b>0.963</b>	0.911
$t_{1/2}$ , months	4.9	—

<sup>a</sup>  $U$  = mg cyanidin-3-glucoside equivalent per L (for total monomeric anthocyanins) and  $U$  = absorbance units (for polymeric color);  $k_0$  = zero-order rate constant;  $k_1$  = first-order rate constant;  $R^2$  = coefficient of determination;  $t_{1/2}$  = half-life.

oxidative reactions.<sup>96</sup> The TMA degradation following a first-order kinetics was similar to reports in previous studies on different fruit juices during storage.<sup>53,93,101</sup> The half-life of TMA was estimated at 4.9 months. The polymeric color formation, on the other hand, follows a zero-order kinetic model having a higher coefficient of regression, as shown in Table 6, indicating that polymeric color formation proceeds at a constant rate of 0.130 absorbance units per month. The polymeric color formation following a zero-order kinetics was in agreement with several studies on juices during storage.<sup>94,96</sup> The estimated half-life for polymeric color formation was 2.8 months.

### 3.7 Microbiological quality of cranberry juice before FO and during refrigerated storage

The cranberry juice before FO and the RO + FO concentrate were evaluated for total plate counts (TPC) and yeast & mold counts (Y&M). Before FO processing, the TPC was  $1.34 \pm 0.31$  log CFU mL<sup>-1</sup> and remained at the same level after FO concentration. No reduction occurred during FO since the juice was processed at room temperature. A reduction in the TPC was observed after 1 month of refrigerated storage to  $1.24 \pm 0.33$  log CFU mL<sup>-1</sup>. The TPC counts were below the level of detection (<1.0 log CFU mL<sup>-1</sup>) after 3 months and remained undetectable after 6



months of refrigerated storage. Y&M was undetectable ( $<1.0 \text{ log CFU mL}^{-1}$ ) before and after FO processing and during the refrigerated shelf-life. The reduction in TPC during refrigerated storage could be attributed to the intrinsic properties of the juice. It has been reported in several studies that cranberry juice concentrate has antibacterial activity and the reduction in microbial counts could be due to the synergistic effect of low pH and the presence of phenolic compounds.<sup>102–104</sup>

## 4 Conclusion

A sequential RO and FO process successfully concentrated cranberry juice to 52° Brix. At least 87% of total phenolics and total flavonoid contents were retained during refrigerated storage compared to thermal concentration where up to 89% of cranberry juice phenolics were degraded,<sup>9</sup> offering superior nutritional quality. Most quality attributes were also retained but there were observable changes in color and the degradation of anthocyanins was evident during refrigerated storage. Though the anthocyanins were mostly retained during the RO and FO processes, the losses during refrigerated storage suggest that frozen storage (below  $-18^\circ\text{C}$ ), which is a typical storage condition for most juice concentrates, may be necessary for the product to maintain high quality,<sup>105</sup> even though the RO + FO cranberry juice concentrate was microbiologically stable for 6 months. Further studies are needed to compare the quality and stability of nonthermally and thermally concentrated cranberry juice, and to assess the feasibility of a large-scale setup, considering that this study utilized a pilot RO and benchtop FO units.

## Author contributions

Mark Emile H. Punzalan: conceptualization, methodology, formal analysis, investigation, visualization, writing – original draft, writing – review & editing. Olga I. Padilla-Zakour: conceptualization, methodology, writing – review & editing, supervision, funding acquisition.

## Conflicts of interest

The authors declare that they have no known competing financial interests or personal relationships that could have appeared to influence the work reported in this paper.

## Data availability

The authors confirm that the data supporting the findings of this study are available and presented within the article. The authors can be contacted for data sharing and further information.

## Acknowledgements

This study was funded by USDA National Institute of Food and Agriculture Grant No. 2019-68015-29228. The authors would like to thank Ocean Spray (Middleborough, MA, USA) for the

cranberry juice used in this study; Roger Morse, Robert Martin, and George Howick for their assistance during pilot plant operations; the Cornell Craft Beverage Analytical Lab for organic acids testing; Cornell Food Microbiology Lab for technical assistance during microbiological analyses; and Dr Chang Chen for his invaluable insights.

## References

- 1 G. Williams, C. I. Stothart, D. Hahn, J. H. Stephens, J. C. Craig and E. M. Hodson, *Cochrane Database Syst. Rev.*, 2023, **11**(11), CD001321.
- 2 E. Pappas and K. M. Schaich, *Crit. Rev. Food Sci. Nutr.*, 2009, **49**, 741–781.
- 3 S. Caillet, J. Côté, G. Doyon, J.-F. Sylvain and M. Lacroix, *Food Res. Int.*, 2011, **44**, 1408–1413.
- 4 G. Cásedas, F. Les, M. Pilar Gómez-Serranillos, C. Smith and V. López, *Food Funct.*, 2017, **8**, 4187–4193.
- 5 B. V. Nemzer, F. Al-Taher, A. Yashin, I. Revelsky and Y. Yashin, *Molecules*, 2022, **27**, 1503.
- 6 L. Dumitrașcu, I. Banu, L. Patrașcu, I. Vasilean and I. Aprodu, *Appl. Sci.*, 2024, **14**, 8713.
- 7 B. P. Mahanta, P. K. Bora, P. Kemprai, G. Borah, M. Lal and S. Haldar, *Food Res. Int.*, 2021, **145**, 110404.
- 8 F. N. Vieira, S. Lourenço, L. G. Fidalgo, S. A. O. Santos, A. J. D. Silvestre, E. Jerónimo and J. A. Saraiva, *Molecules*, 2018, **23**, 2706.
- 9 J. Côté, S. Caillet, D. Dussault, J.-F. Sylvain and M. Lacroix, *Food Res. Int.*, 2011, **44**, 2922–2929.
- 10 M. U. Khan, K. Hamid, I. Tolstorebrev and T. M. Eikevik, *Food Chem.*, 2024, **452**, 139559.
- 11 O. Miyawaki and T. Inakuma, *Food Bioprocess Technol.*, 2021, **14**, 39–51.
- 12 F. G. F. Qin, Z. Ding, K. Peng, J. Yuan, S. Huang, R. Jiang and Y. Shao, *J. Food Eng.*, 2021, **291**, 110270.
- 13 K. D. P. P. Gunathilake, L. J. Yu and H. P. V. Rupasinghe, *Food Chem.*, 2014, **148**, 335–341.
- 14 S. Álvarez, F. A. Riera, R. Álvarez and J. Coca, *Ind. Eng. Chem. Res.*, 2002, **41**, 6156–6164.
- 15 P. D. Gurak, L. M. C. Cabral, M. H. M. Rocha-Leão, V. M. Matta and S. P. Freitas, *J. Food Eng.*, 2010, **96**, 421–426.
- 16 R. Garud, S. Kore, V. Kore and G. Kulkarni, *Univers. J. Environ. Res. Technol.*, 2011, **1**, 233–238.
- 17 I. G. Wenten, *Desalination*, 2016, **391**, 112–125.
- 18 B. Jiao, A. Cassano and E. Drioli, *J. Food Eng.*, 2004, **63**, 303–324.
- 19 I. B. Aguiar, N. G. M. Miranda, F. S. Gomes, M. C. S. Santos, D. de G. C. Freitas, R. V. Tonon and L. M. C. Cabral, *Innovative Food Sci. Emerging Technol.*, 2012, **16**, 137–142.
- 20 D. S. Couto, L. M. C. Cabral, V. M. Da Matta, R. Deliza and D. D. C. Freitas, *Cienc. Tecnol. Aliment.*, 2011, **31**, 905–910.
- 21 F. Dos Santos Gomes, P. A. Da Costa, M. B. D. De Campos, S. Couri and L. M. C. Cabral, *Desalin. Water Treat.*, 2011, **27**, 120–122.
- 22 A. P. Echavarria, V. Falguera, C. Torras, C. Berdún, J. Pagán and A. Ibarz, *LWT–Food Sci. Technol.*, 2012, **46**, 189–195.



23 D. F. Jesus, M. F. Leite, L. F. M. Silva, R. D. Modesta, V. M. Matta and L. M. C. Cabral, *J. Food Eng.*, 2007, **81**, 287–291.

24 V. M. Matta, R. H. Moretti and L. M. C. Cabral, *J. Food Eng.*, 2004, **61**, 477–482.

25 N. Pap, S. Kertész, E. Pongrácz, L. Myllykoski, R. L. Keiski, G. Vatai, Z. László, S. Beszédes and C. Hodúr, *Desalination*, 2009, **241**, 256–264.

26 K. D. P. P. Gunathilake, H. P. V. Rupasinghe and N. L. Pitts, *Food Res. Int.*, 2013, **52**, 535–541.

27 A. Achilli, T. Y. Cath and A. E. Childress, *J. Membr. Sci.*, 2010, **364**, 233–241.

28 N. K. Rastogi, *Crit. Rev. Food Sci. Nutr.*, 2016, **56**, 266–291.

29 H. Wang, Y. Zhang, S. Ren, J. Pei and Z. Li, *Chem. Eng. Res. Des.*, 2022, **177**, 569–577.

30 H. M. Tavares, I. C. Tessaro and N. S. M. Cardozo, *Innovative Food Sci. Emerging Technol.*, 2022, **75**, 102905.

31 D. Trishitman, P. S. Negi and N. K. Rastogi, *Food Chem.*, 2023, **399**, 133972.

32 H. N. Shalini and C. A. Nayak, in *Recent Advances in Chemical Engineering*, Springer, 2016, pp. 81–88.

33 H. Q. Chu, Z. H. Zhang, H. Z. Zhong, K. Yang, P. L. Sun, X. J. Liao and M. Cai, *Membranes*, 2022, **12**, 808.

34 Q. Ge, M. Ling and T.-S. Chung, *J. Membr. Sci.*, 2013, **442**, 225–237.

35 K. Zhang, X. An, Y. Bai, C. Shen, Y. Jiang and Y. Hu, *J. Membr. Sci.*, 2021, **635**, 119495.

36 M. E. H. Punzalan, P. A. Marcelo and O. I. Padilla-Zakour, *LWT-Food Sci. Technol.*, 2025, **223**, 117693.

37 S. Zhao, L. Zou, C. Y. Tang and D. Mulcahy, *J. Membr. Sci.*, 2012, **396**, 1–21.

38 Y. Chun, D. Mulcahy, L. D. Zou and I. S. Kim, *Membranes*, 2017, **7**, 30.

39 N. Akther, A. Sodiq, A. Giwa, S. Daer, H. A. Arafat and S. W. Hasan, *Chem. Eng. J.*, 2015, **281**, 502–522.

40 United States Department of Agriculture, *Food Data Central*, 2019, <https://fdc.nal.usda.gov/food-details/2003594/nutrients>.

41 S. L. Brown, K. M. Leonard and S. L. Messimer, *Ozone:Sci. Eng.*, 2008, **30**, 152–164.

42 D. L. Quoc, T. D. N. Thuc and D. N. Hoang, *J. Food Process Eng.*, 2022, **45**, e14183.

43 E. M. Garcia-Castello, L. Mayor, S. Chorques, A. Argüelles, D. Vidal-Brotons and M. L. Gras, *J. Food Eng.*, 2011, **106**, 199–205.

44 A. A. Beldie and C. I. Moraru, *J. Dairy Sci.*, 2021, **104**, 7522–7533.

45 A. A. Beldie, J. Dumpler and C. I. Moraru, *J. Food Eng.*, 2025, **400**, 112655.

46 Alfa Laval, *Membrane Filtration System HMI Operation Manual*, 2018.

47 AOAC International, *Official Methods of Analysis of AOAC International*, AOAC International, Gaithersburg, MD, USA, 21st edn, 2019.

48 M. R. Dorris, D. M. Voss, M. A. Bollom, M. P. Krawiec-Thayer and B. W. Bolling, *J. Food Sci.*, 2018, **83**, 911–921.

49 A. L. Waterhouse, *Curr. Protoc.*, 2002, **6**, 1–8.

50 J. Lee, R. W. Durst and R. E. Wrolstad, *J. AOAC Int.*, 2005, **88**, 1269–1278.

51 D. Nowak, M. Goślinśki and L. Kłębukowska, *Plant Foods Hum. Nutr.*, 2022, **77**, 427–435.

52 R. Re, N. Pellegrini, A. Proteggente, A. Pannala, M. Yang and C. Rice-Evans, *Free Radical Biol. Med.*, 1999, **26**, 1231–1237.

53 J. Chen, J. Du, M. Li and C. Li, *LWT-Food Sci. Technol.*, 2020, **128**, 109448.

54 M. R. Sohrabi, S. S. Madaeni, M. Khosravi and A. M. Ghaedi, *Sep. Purif. Technol.*, 2010, **75**, 121–126.

55 S. Sridhar, A. Kale and A. A. Khan, *J. Membr. Sci.*, 2002, **205**, 83–90.

56 Q. Ma, Q. Lei, F. Liu, Z. Song, B. Khusid and W. Zhang, *Water Environ. Res.*, 2024, **96**, e10983.

57 S. S. Madaeni and Y. Mansourpanah, *Desalination*, 2004, **161**, 13–24.

58 P. Menchik and C. I. Moraru, *J. Food Eng.*, 2019, **253**, 40–48.

59 D. M. Davenport, C. L. Ritt, R. Verbeke, M. Dickmann, W. Egger, I. F. J. Vankelecom and M. Elimelech, *J. Membr. Sci.*, 2020, **610**, 118268.

60 A. Artemi, G. Q. Chen, S. E. Kentish and J. Lee, *J. Membr. Sci.*, 2020, **611**, 118357.

61 C. Lu, Y. Bao and J.-Y. Huang, *Curr. Opin. Food Sci.*, 2021, **42**, 76–85.

62 I. G. Wenten, K. Khoiruddin, R. Reynard, G. Lugito and H. Julian, *J. Food Eng.*, 2021, **290**, 110216.

63 Z. Li, C. Wu, J. Huang, R. Zhou and Y. Jin, *Membranes*, 2021, **11**, 611.

64 D. I. Kim, G. Gwak, M. Zhan and S. Hong, *J. Membr. Sci.*, 2019, **578**, 53–60.

65 Z. Li, S. Xiao, Q. Xiong, C. Wu, J. Huang, R. Zhou and Y. Jin, *J. Food Eng.*, 2022, **333**, 111122.

66 D. Trishitman, P. S. Negi and N. K. Rastogi, *LWT-Food Sci. Technol.*, 2021, **145**, 111522.

67 S.-J. You, X.-H. Wang, M. Zhong, Y.-J. Zhong, C. Yu and N.-Q. Ren, *Chem. Eng. J.*, 2012, **198–199**, 52–60.

68 S. A. F. Zhao and L. D. Zou, *J. Membr. Sci.*, 2011, **379**, 459–467.

69 W. Jiang, X. Xu, L. Lin, H. Wang, R. Shaw, D. Lucero and P. Xu, *Water*, 2019, **11**, 1015.

70 M. Rouina, H.-R. Kariminia, S. A. Mousavi and E. Shahryari, *Desalination*, 2016, **395**, 41–45.

71 D. Trishitman, *J. Food Eng.*, 2025, **399**, 112622.

72 M. Qasim, F. W. Khudhur, A. Aidan and N. A. Darwish, *Ultrason. Sonochem.*, 2020, **61**, 10.

73 B. S. Chanukya and N. K. Rastogi, *Ultrason. Sonochem.*, 2017, **34**, 426–435.

74 R. R. Milczarek, C. W. Olsen and I. Sedej, *Processes*, 2020, **8**, 1568.

75 N. J. Weaver, G. S. Wilkin, K. R. Morison and M. J. Watson, *J. Food Eng.*, 2020, **273**, 109823.

76 O. Bakajin, J. Klare and I. Sedej, *Energy Savings through Osmotic Concentration for the Food Industry*, California Energy Commission, 2023.

77 H. Julian, P. Lestari, I. G. Wenten and K. Khoiruddin, *J. Eng. Technol. Sci.*, 2025, **57**, 214–242.



78 D. Patel, D. Ankoliya, M. Raninga, A. Mudgal, V. Patel, J. Patel, V. Mudgal and H. Choksi, *Environ. Sci. Pollut. Res.*, 2022, **30**, 32108–32116.

79 A. A. Prestes, C. V. Helm, E. A. Esmerino, R. Silva, A. G. da Cruz and E. S. Prudencio, *J. Food Sci.*, 2022, **87**, 488–502.

80 B. Enaru, G. Dreñcanu, T. D. Pop, A. Stănilă and Z. Diaconeasa, *Antioxidants*, 2021, **10**, 1967.

81 M. M. Pagani, M. H. Rocha-Leão, A. B. B. Couto, J. P. Pinto, A. O. Ribeiro, F. d. S. Gomes and L. M. C. Cabral, *Desalination Water Treat.*, 2011, **27**, 130–134.

82 S. Bánvölgyi, S. Horváth, É. Stefanovits-Bányai, E. Békássy-Molnár and G. Vatai, *Desalination*, 2009, **241**, 281–287.

83 Z. Molnár, S. Bánvölgyi, Á. Kozák, I. Kiss, E. Békássy-Molnár and G. Vatai, *Acta Aliment.*, 2012, **41**, 147–159.

84 I. Santana, L. Cabral, V. Matta, M. Araújo, A. Gouvêa and R. Godoy, *Acta Hortic.*, 2014, 281–288.

85 M. H. Choi, G. H. Kim and H. S. Lee, *Food Res. Int.*, 2002, **35**, 753–759.

86 Zs. Cserhalmi, Á. Sass-Kiss, M. Tóth-Markus and N. Lechner, *Innovative Food Sci. Emerging Technol.*, 2006, **7**, 49–54.

87 K. Torskangerpoll and Ø. M. Andersen, *Food Chem.*, 2005, **89**, 427–440.

88 M. V. Gerald, C. B. Betim Cazarin, F. L. Dias-Audibert, G. A. Pereira, G. G. Carvalho, D. Y. Kabuki, R. R. Catharino, G. M. Pastore, J. H. Behrens, M. Cristianini and M. R. Maróstica Júnior, *LWT-Food Sci. Technol.*, 2021, **139**, 110548.

89 L. Yuan, F. Cheng, J. Yi, S. Cai, X. Liao, F. Lao and L. Zhou, *Food Chem.*, 2022, **373**, 131397.

90 I. O. Vvedenskaya and N. Vorsa, *Plant Sci.*, 2004, **167**, 1043–1054.

91 M. J. Rein and M. Heinonen, *J. Agric. Food Chem.*, 2004, **52**, 3106–3114.

92 C. M. B. Neves, A. Pinto, F. Gonçalves and D. F. Wessel, *Appl. Sci.*, 2021, **11**, 6941.

93 A. Wojdylo, P. Nowicka and M. Teleszko, *Processes*, 2019, **7**, 367.

94 A. Martynenko and Y. Chen, *J. Food Eng.*, 2016, **171**, 44–51.

95 T. Jiang, Y. Mao, L. Sui, N. Yang, S. Li, Z. Zhu, C. Wang, S. Yin, J. He and Y. He, *Food Chem.*, 2019, **274**, 460–470.

96 M. Türkyılmaz and M. Özkan, *Int. J. Food Sci. Technol.*, 2012, **47**, 2273–2281.

97 A. Bermejo-Prada and L. Otero, *J. Food Eng.*, 2016, **169**, 141–148.

98 B. M. Muche, R. A. Speers and H. P. V. Rupasinghe, *Front. Nutr.*, 2018, **5**, 1–9.

99 A. Navruz, M. Türkyılmaz and M. Özkan, *Food Chem.*, 2016, **197**, 150–160.

100 M. R. Dorris and B. W. Bolling, *Antioxidants*, 2021, **10**, 1788.

101 T. Boranbayeva, F. Karadeniz and E. Yilmaz, *Food Bioprocess Technol.*, 2014, **7**, 1894–1902.

102 M. Daoutidou, S. Plessas, A. Alexopoulos and I. Mantzourani, *Foods*, 2021, **10**, 486.

103 M. Harich, B. Maherani, S. Salmieri and M. Lacroix, *Food Control*, 2017, **75**, 134–144.

104 M. C. L. Nogueira, O. A. Oyarzábal and D. E. Gombas, *J. Food Prot.*, 2003, **66**, 1637–1641.

105 A. Adnan, M. Mushtaq and T. ul Islam, in *Fruit Juices*, ed. B. K. Tiwari, Academic Press, San Diego, 2018, pp. 217–240.

